Azimuthal correlations in Z+jet events at high transverse momentum calculated at next-to-leading order in the parton branching method

H. Yang, A. Bermudez Martinez, F. Hautmann, H. Jung, M. Mendizabal, S. Taheri Monfared, S. Prestel, Q. Wang, K. Wichmann

March 16, 2022

Abstract

The predictions of azimuthal correlations in Z+jet production are compared with those for multijet production in the same kinematic range by applying Parton - Branching TMD distributions to NLO calculations via MCatNLO supplemented by PB-TMD parton showers. The azimuthal correlations $\Delta\phi_{12}$, obtained in Z+jet production are steeper compared to those in multijet production at transverse momenta $p_{\mathrm{T}}^{\mathrm{leading}} \sim 200$ GeV, while they become similar for very high transverse momenta, $p_{\mathrm{T}}^{\mathrm{leading}} \sim 1000$ GeV, coming from the initial parton configuration of both processes.

In Z+jet production the colored partonic final state is different compared to the one in multijet production and differences in the azimuthal correlations can be also attributed to potential *factorization - breaking* effects. In order to experimentally investigate those effects, we propose to measure the ratio of the distributions in $\Delta\phi_{12}$ for Z+jet- and multijet production at low and at very high $p_{\mathrm{T}}^{\mathrm{leading}}$, and compare those to predictions obtained assuming factorization.

1 Introduction

The description of the cross section of high p_{T} jets in association with a Z-boson at high p_{T} in proton-proton (pp) collisions is an important test for predictions obtained in Quantum Chromodynamics (QCD). At leading order in the strong coupling α_{s}, the azimuthal angle $\Delta\phi_{12}$ between the Z-boson and the jet is $\Delta\phi_{12} = \pi$, and a deviation from this back-to-back scenario is a measure of higher order radiation. In multijet events the azimuthal correlation between two jets has been measured at the LHC by ATLAS and CMS [1–5]. The production of Z bosons associated with jets has been measured at lower energies, by CDF and D0 in proton-antiproton ($\mathrm{p\bar{p}}$) collisions at a center-of-mass energy $\sqrt{s} = 1.96$ GeV [6, 7]. At the LHC the ATLAS and CMS collaborations have published measurements in pp collisions at a center-of-mass energy $\sqrt{s} = 7$ TeV [8–10], 8 TeV [11] and 13 TeV [12, 13]. The azimuthal correlation between Z-bosons and jets has been measured at 8 TeV [11] and 13 TeV [13]. However, all the measurements of azimuthal correlations were performed at rather low transverse momenta of the Z-boson and the jets ($p_{\mathrm{T}} < \mathcal{O}(100)$ GeV), where multiparton emissions are signifiant and next-to-leading (NLO) calculations of Z+jet are not sufficient to describe the measurement. With the increase of luminosity at the LHC, it becomes possible to measure Z+jet production in the high p_{T} range, with $p_{\mathrm{T},Z} > \mathcal{O}(100)$ GeV. In this high p_{T} region, NLO calculations become appropriate, and especially the back-to-back region can be studied in detail, which gives important information on soft gluon resummation and effects of the transverse momenta of the initial partons in form of transverse momentum dependent (TMD) parton distributions.

In a previous publication [14] we have investigated the $\Delta\phi_{12}$ correlation in high-p_{T} dijet events by applying TMDs together with next-to-leading order calculations of the hard scattering process. The application of TMDs allows a direct investigation of initial state parton radiation (for an overview on TMDs see [15]). While hard perturbative higher order radiation leads to a large azimuthal decorrelation ($\Delta\phi_{12} < \pi$), soft multi-gluon emissions, which cannot be described by fixed order calculations, dominate in the region $\Delta\phi_{12} \to \pi$. The region of $\Delta\phi_{12} \to \pi$ is of special interest, since so-called *factorization - breaking* [16–18] effects could become important in case of colored final states. Multijet production is believed to be sensitive to such effects, and to a lesser extend also Z+jet production, because of the presence of the Z-boson. In order to investigate factorization - breaking effects, we propose to compare the theoretical description of the azimuthal correlation $\Delta\phi_{12}$ in multijet production with the one in Z+jet production.

In this letter we compare in detail high-p_{T} dijet and Z+jet production by applying the Parton Branching (PB) formulation of TMD evolution [19,20] together with NLO calculations of the hard scattering process in the MADGRAPH5_AMC@NLO [21] framework. In Ref. [14] these PB TMD parton distributions were applied to multijet production at large transverse momenta. We apply the same method to the calculation of Z+jet production. We propose to use the same kinematic region for the high-p_{T} dijet and Z+jet production to allow a direct comparison of the measurement. At large enough p_{T} the mass of the Z-boson becomes negligible, and the different color structure of the final states might allow to observe factorization - breaking effects by comparing the measurements to calculations assuming factorization.

2 Calculation of Z+jet distributions

The PB - method to solve the DGLAP [22–25] evolution equation is described in Ref. [19,20] and the NLO PB collinear and TMD parton distribution were obtained in Ref. [26] from QCD fits to precision DIS data from at HERA [27]. The process Z+jet at NLO is calculated with MADGRAPH5_AMC@NLO using the collinear PB-NLO-2018-Set 2, as obtained in Ref. [26] applying $\alpha_{\mathrm{s}}(M_{\mathrm{Z}}) = 0.118$. The same procedure as described for the case of multijet production [14] is applied, and predictions are obtained by processing the MADGRAPH5_AMC@NLO event files in LHE format [28] through CASCADE33 [29] for an inclusion of TMD effects in the initial state and for simulation of the corresponding parton shower.

Fixed order NLO Z+jet production is calculated with MADGRAPH5_AMC@NLO in a procedure similar to the one applied for dijet production described in [14]. For the MC@NLO mode, the HERWIG6 [30,31] subtraction terms are calculated, as they are best suited for the use with PB - parton densities, because both apply a similar angular ordering condition. The matching scale $\mu_m = \mathtt{SCALUP}$ limits the contribution from PB-TMDs and TMD showers.

In the NLO calculations the factorization and renormalization scales are set to $\mu_{R,F} = \frac{1}{2}\sum_i p_{\mathrm{T},i}$, where the index i runs over all particles in the matrix element final state. This scale is also used as μ in the PB-TMD parton distribution $\mathcal{A}(x, k_{\mathrm{T}}, \mu)$. The scale uncertainties of the predictions are obtained from variations of the scales around the central value in the 7-point scheme avoiding extreme cases of variation.

In Fig. 1 we show the distributions of the transverse momentum of the Z+jet-system, $p_{\mathrm{T},Zj}$, and the azimuthal correlation in the Z+jet-system, $\Delta\phi_{\mathrm{Zj}}$, for a fixed NLO calculation, as well as for the full simulation including PB-TMDs and parton showers. We require a

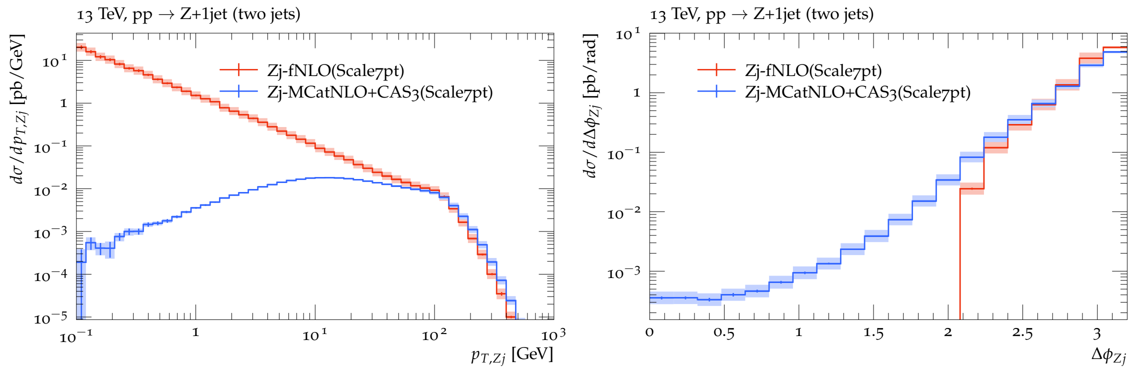

Figure 1: Transverse momentum spectrum of the Z+jet-system $p_{\mathrm{T},Zj}$ (left) and $\Delta\phi_{\mathrm{Zj}}$ distribution (right). The predictions are shown for fixed NLO (MCatNLO(fNLO) and after inclusion of PB-TMDs (MCatNLO+CAS3).

transverse momentum $p_{\mathrm{T}} > 200$ GeV for the Z-boson and define jets with the anti-k_{T} jet-algorithm [32], as implemented in the FASTJET package [33], with a distance parameter of R=0.4.

In the low $p_{\mathrm{T},Zj}$-region one can clearly see the expected divergent behavior of the fixed NLO prediction. In the $\Delta\phi_{\mathrm{Zj}}$ distribution one can observe the limited region for fixed NLO at $\Delta\phi_{\mathrm{Zj}} < 2/3\pi$, since at most two jets in addition to the Z-boson appear in the calculation. At large $\Delta\phi_{\mathrm{Zj}}$, the fixed NLO prediction rises faster than the full calculation including resummation via PB-TMDs and parton showers.

3 Azimuthal correlations in $\mathrm{Z}+$jet and multijet production

We now apply predictions obtained in the framework described above to Z+jet and multijet production. We use the same kinematic region as described in the measurement of the azimuthal correlations $\Delta\phi_{12}$ in multijet production obtained by CMS at $\sqrt{s} = 13$ TeV [4] and in the back-to-back region ($\Delta\phi_{12} \to \pi$) [5].

We consider only Z-bosons leading in p_{T} with a transverse momentum of $p_{\mathrm{T}}^{\mathrm{leading}} > 200$ GeV. We consider distributions of the azimuthal correlation between the Z-boson and the leading jet, $\Delta\phi_{\mathrm{Zj}}$, for $p_{\mathrm{T}}^{\mathrm{leading}} > 200$ GeV as well as for the very high p_{T} region of $p_{\mathrm{T}}^{\mathrm{leading}} >$ 1000 GeV. We apply the collinear and TMD set PB-NLO-2018-Set 2 with running coupling $\alpha_{\mathrm{s}}(m_{\mathrm{Z}}) = 0.118$.

In Fig. 2 we show the predictions for azimuthal correlations $\Delta\phi_{\mathrm{Zj}}$ ($\Delta\phi_{12}$) for Z+jet production and compare also to the measurement and predictions of azimuthal correlations $\Delta\phi_{12}$ in multijet production [4].

In Fig. 3 the predictions for the azimuthal correlations $\Delta\phi_{\mathrm{Zj}}$ ($\Delta\phi_{12}$) for Z+jet (multijet) production in the back-to-back regions are shown and compared to the measurement of dijet

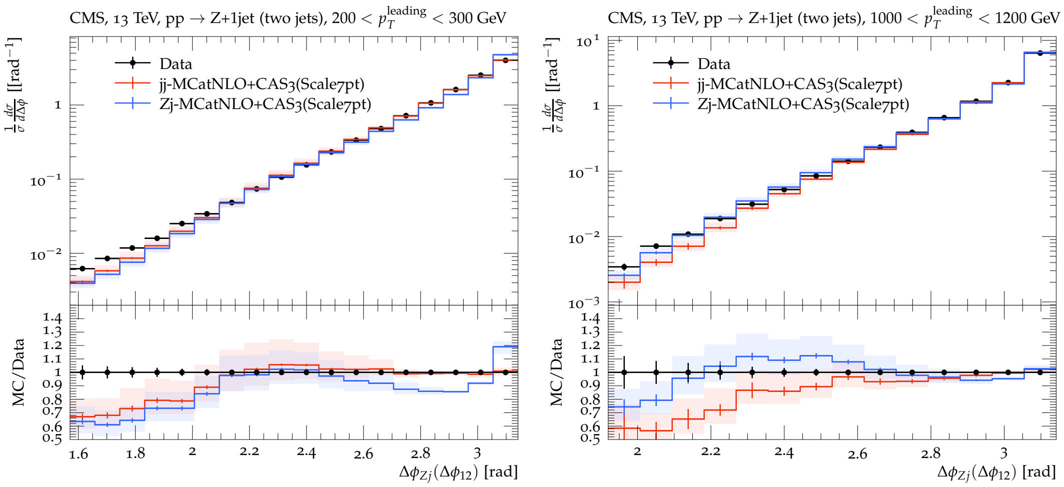

Figure 2: Azimuthal correlation $\Delta\phi_{\mathrm{Zj}}$ ($\Delta\phi_{12}$) for $p_{\mathrm{T}}^{\mathrm{leading}} > 200$ GeV (left) and $p_{\mathrm{T}}^{\mathrm{leading}} > 1000$ GeV (right) as measured by CMS [4] compared with predictions from MCatNLO+CAS3. Shown are the uncertainties coming from the scale variation (as described in the text).

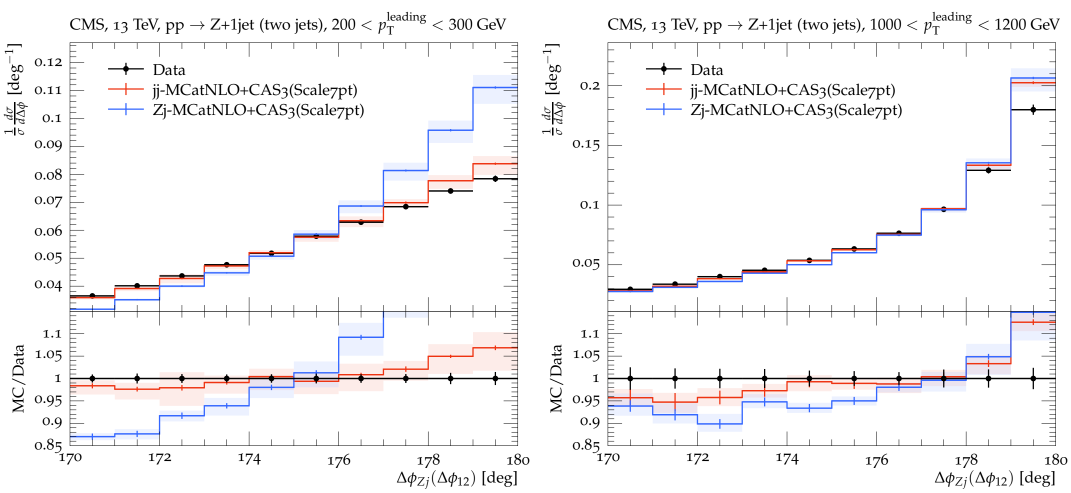

Figure 3: Azimuthal correlation $\Delta\phi_{\mathrm{Zj}}(\Delta\phi_{12})$ in the back-to-back region for $p_{\mathrm{T}}^{\mathrm{leading}} > 200$ GeV (left) and $p_{\mathrm{T}}^{\mathrm{leading}} > 1000$ GeV (right) as measured by CMS [5] compared with predictions from MCatNLO+CAS3. Shown are the uncertainties coming from the scale variation (as described in the text).

production of CMS [5]. We observe, that the distribution of azimuthal angle $\Delta\phi_{\mathrm{Zj}}$ in Z+jet-production for $p_{\mathrm{T}}^{\mathrm{leading}} > 200$ GeV is more strongly correlated toward π than the distribution of angle $\Delta\phi_{12}$ in multijet production. This difference is washed out for $p_{\mathrm{T}}^{\mathrm{leading}} > 1000$ GeV.

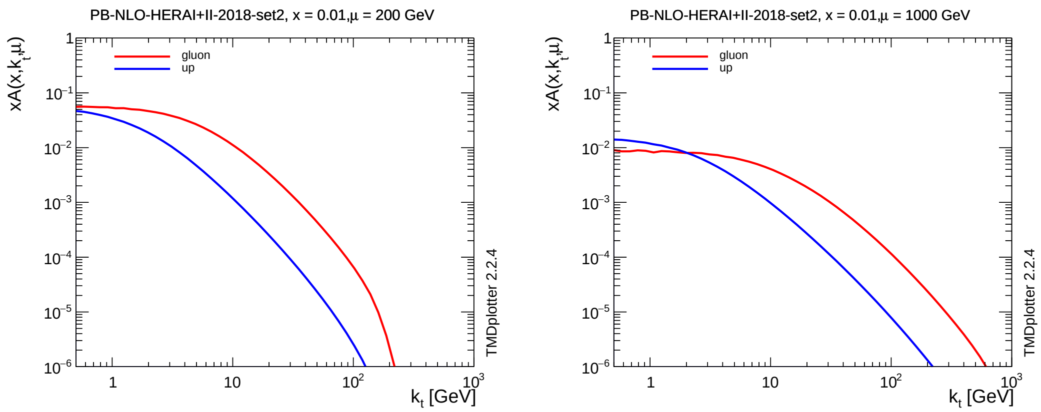

Figure 4: TMD parton density distributions for up quarks (PB-NLO-2018-Set 2) as a function of k_{T} at $\mu = 200$ and 1000 GeV and $x = 0.01$.

Differences in $\Delta\phi$ between Z+jet and multijet production can result from the different flavor composition of the initial state and therefore different initial state transverse momenta and initial state parton shower, as well as from differences in final state showering since both processes have different numbers of colored final state partons. Effects coming from factorization - breaking, interactions between initial and final state partons, will certainly depend on the final structure and the number of colored final state partons.

We first investigate the role of initial state radiation and the dependence on the transverse momentum distributions coming from the TMDs, which gives a large contribution to the decorrelation in $\Delta\phi$. The k_{T}-distribution obtained from a gluon TMD is different from the one of a quark TMD as shown in Fig. 4 for $x = 0.01$ and scales of $\mu = 200(1000)$ GeV. In Fig. 5 we show the probability of gg, qg and qq initial states (q stands for quark and antiquark) as a function of $p_{\mathrm{T}}^{\mathrm{leading}}$ for Z+jet and multijet production. At high $p_{\mathrm{T}}^{\mathrm{leading}} > 1000$ GeV the qq channel is dominant for both Z+jet and multijet final states, while at lower $p_{\mathrm{T}}^{\mathrm{leading}} > 200$ GeV the gg channel is dominant in multijet production, leading to larger decorrelation effects, since gluons radiate more compared to quarks.

The role of final state radiation in the correlation in $\Delta\phi_{12}$ distributions is more difficult to estimate, since the subtraction terms for the NLO matrix element calculation also depend on the structure of the final state parton shower. In order to estimate the effect of final state shower we compare a calculation of the azimuthal correlations in the back-to-back region obtained with MCatNLO+CAS3 with the one obtained with MCatNLO+PYTHIA8. For the calculation MCatNLO+PYTHIA8 we apply the PYTHIA8 subtraction terms in the MADGRAPH5_AMC@NLOcalculation, use the NNPDF3.0 [34] parton density and tune CUETP8M1 [35].

As shown in Fig. 6, the distributions are different because of the different parton shower

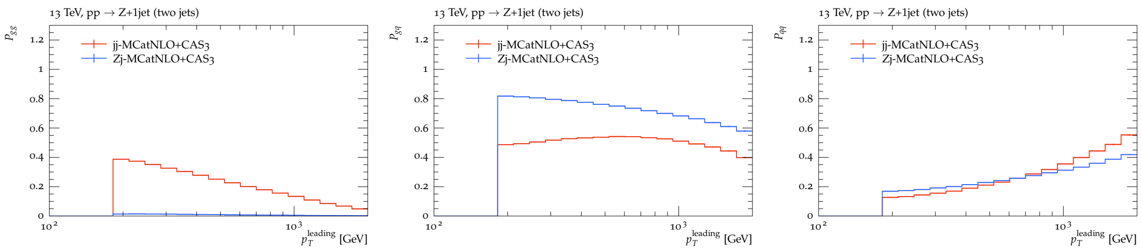

Figure 5: The probability of gg, qg and qq initial states in Z+jet and multijet production (q stands for quark and antiquark).

in CASCADE3 and PYTHIA8, but the ratio of the distributions for Z+jet and multijet production are similar: Z+jet-production gives a steeper (more strongly correlated) distribution at low $p_{\mathrm{T}}^{\mathrm{leading}}$, while at high $p_{\mathrm{T}}^{\mathrm{leading}}$ the distributions become similar in shape.

The matching scale μ_m limits the hardness of parton-shower emissions, and is thus typically a non-negligible source of variation in matched calculations (see e.g. [36] for a detailed discussion). It is thus interesting to assess the robustness of the previous findings under matching scale variation. Assessing matching scale variations in both an angular-ordered shower – such as CASCADE3 – and a transverse-momentum-ordered shower – such as PYTHIA8 – additionally tests the *interpretation* of the matching scale: In an angular-ordered shower, the matching scale is applies as "veto scale" applied to avoid larger transverse momenta for *any* emission, while in transverse-momentum ordered showers, the matching scale sets the maximal transverse momentum of the *first* shower emission. The result of changing the matching scale to half of twice the central value is shown in Fig. 7. As expected, the value of the matching scale has a large impact on the prediction. This is particularly apparent when μ_m is used to set the maximal transverse momemtum of the first emission in PYTHIA8. Overall, we find that interpreting the matching scale as veto scale in CASCADE3 leads to more robust predictions. Interestingly, the matching scale uncertainty seems to improve for higher-p$_T^{\mathrm{leading}}$ jet configurations in CASCADE3.

In order to measure experimentally effects which could originate from factorization - breaking at the back-to-back region we propose to measure the ratio of distributions in $\Delta\phi_{12}$ for Z+jet- and multijet production at low and very high $p_{\mathrm{T}}^{\mathrm{leading}}$, and compare the measurement with predictions assuming factorization. Since the parton configuration of both processes becomes similar at high $p_{\mathrm{T}}^{\mathrm{leading}}$, differences of the ratio from predictions could hint on possible factorization - breaking effects.

4 Summary and conclusions

We have investigated azimuthal correlations in Z+jet- production and compared predictions with those for multijet production in the same kinematic range. The predictions are based on

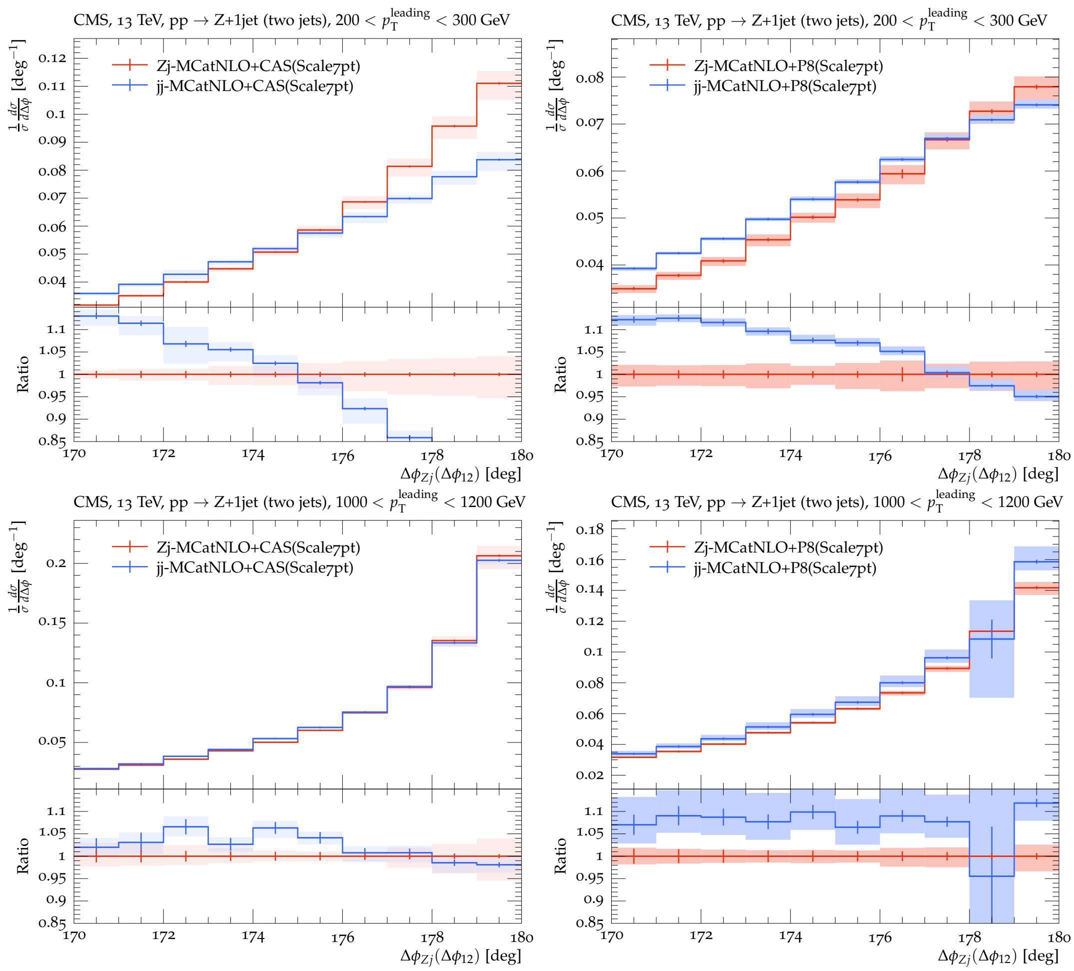

Figure 6: Azimuthal correlation $\Delta\phi_{\mathrm{Zj}}(\Delta\phi_{12})$ in the back-to-back region for $p_{\mathrm{T}}^{\mathrm{leading}} > 200$ GeV (upper row) and $p_{\mathrm{T}}^{\mathrm{leading}} > 1000$ GeV (lower row) compared with predictions obtained with MCatNLO+CAS3 (left column) and obtained with MCatNLO+PYTHIA8 (right column).

PB-TMD distributions with NLO calculations via MCatNLO supplemented by PB-TMD parton showers via CASCADE3. The azimuthal correlations $\Delta\phi_{12}$, obtained in Z+jet-production are steeper compared to those in multijet production at transverse momenta $p_{\mathrm{T}}^{\mathrm{leading}} \sim 200$ GeV, while they become similar for very high transverse momenta, $p_{\mathrm{T}}^{\mathrm{leading}} \sim 1000$ GeV, coming from the initial parton configuration of both processes.

In Z+jet production the colored partonic final state is different compared to the one in multijet production and differences in the azimuthal correlations can be also attributed to potential factorization - breaking effects. In order to experimentally investigate those ef-

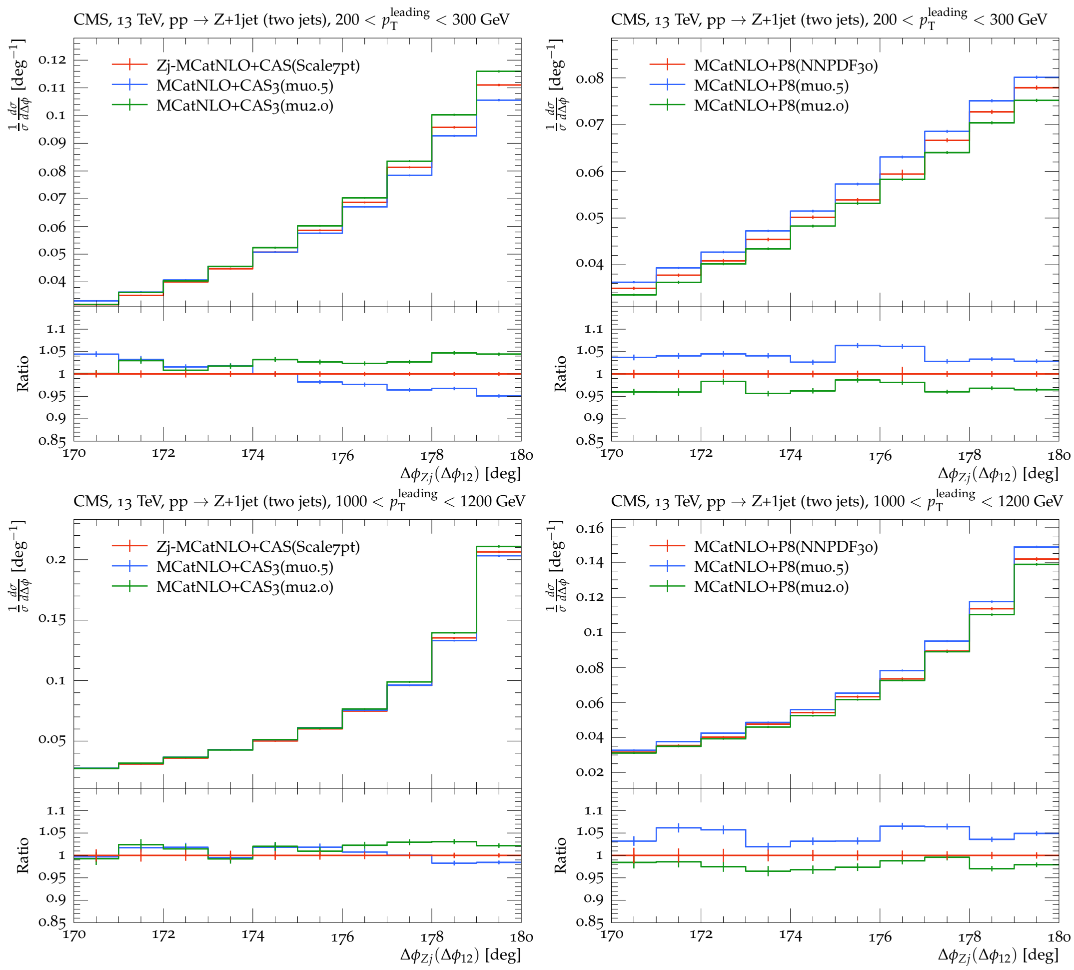

Figure 7: Azimuthal correlation $\Delta\phi_{\mathrm{Zj}}(\Delta\phi_{12})$ in the back-to-back region for $p_{\mathrm{T}}^{\mathrm{leading}} > 200$ GeV (upper row) and $p_{\mathrm{T}}^{\mathrm{leading}} > 1000$ GeV (lower row) compared with predictions obtained with MCatNLO+CAS3 (left column) and obtained with MCatNLO+PYTHIA8 (right column).

fects, we propose to measure the ratio of the distributions in $\Delta\phi_{12}$ for Z+jet- and multijet production at low and at very high $p_{\mathrm{T}}^{\mathrm{leading}}$, and compare those to predictions obtained assuming factorization.

Acknowledgments.
We are grateful to Olivier Mattelaer from the MADGRAPH5_AMC@NLO team for discussions, help and support with the lhe option for fixed NLO calculations in MCatNLO.

References

[1] ATLAS Collaboration, "Measurement of dijet azimuthal decorrelations in pp collisions at sqrt(s)=7 TeV", *Phys.Rev.Lett.* **106** (2011) 172002, `arXiv:1102.2696`.

[2] CMS Collaboration, "Dijet Azimuthal Decorrelations in pp Collisions at sqrt(s) = 7 TeV", *Phys. Rev. Lett.* **106** (2011) 122003, `arXiv:1101.5029`.

[3] CMS Collaboration, "Measurement of dijet azimuthal decorrelation in pp collisions at $\sqrt{s} = 8\,\mathrm{TeV}$", *Eur. Phys. J. C* **76** (2016) 536, `arXiv:1602.04384`.

[4] CMS Collaboration, "Azimuthal correlations for inclusive 2-jet, 3-jet, and 4-jet events in pp collisions at $\sqrt{s} = 13$ TeV", *Eur. Phys. J.* **C78** (2018) 566, `arXiv:1712.05471`.

[5] CMS Collaboration, "Azimuthal separation in nearly back-to-back jet topologies in inclusive 2- and 3-jet events in pp collisions at $\sqrt{s} = 13$ TeV", *Eur. Phys. J. C* **79** (2019) 773, `arXiv:1902.04374`.

[6] CDF Collaboration, "Measurement of inclusive jet cross-sections in $Z/\gamma^* \to e^+e^-$ + jets production in $p\bar{p}$ collisions at $\sqrt{s}$ = 1.96-TeV", *Phys. Rev. Lett.* **100** (2008) 102001, `arXiv:0711.3717`.

[7] D0 Collaboration, "Measurement of differential Z/γ^* + jet + X cross sections in $p\bar{p}$ collisions at $\sqrt{s}$ = 1.96-TeV", *Phys. Lett.* **B669** (2008) 278–286, `arXiv:0808.1296`.

[8] ATLAS Collaboration, "Measurement of the production cross section of jets in association with a Z boson in pp collisions at $\sqrt{s}$ = 7 TeV with the ATLAS detector", *JHEP* **07** (2013) 032, `arXiv:1304.7098`.

[9] ATLAS Collaboration, "Measurement of the production cross section for Z/gamma* in association with jets in pp collisions at $\sqrt{s} = 7$ TeV with the ATLAS detector", *Phys. Rev. D* **85** (2012) 032009, `arXiv:1111.2690`.

[10] CMS Collaboration, "Measurements of jet multiplicity and differential production cross sections of $Z+$ jets events in proton-proton collisions at $\sqrt{s} = 7$ TeV", *Phys. Rev. D* **91** (2015), no. 5, 052008, `arXiv:1408.3104`.

[11] CMS Collaboration, "Measurements of differential production cross sections for a Z boson in association with jets in pp collisions at $\sqrt{s} = 8$ TeV", *JHEP* **04** (2017) 022, `arXiv:1611.03844`.

[12] ATLAS Collaboration, "Measurements of the production cross section of a Z boson in association with jets in pp collisions at $\sqrt{s} = 13$ TeV with the ATLAS detector", *Eur. Phys. J.* **C77** (2017), no. 6, 361, `arXiv:1702.05725`.

[13] CMS Collaboration, “Measurement of differential cross sections for Z boson production in association with jets in proton-proton collisions at $\sqrt{s} = 13$ TeV”, *Eur. Phys. J.* **C78** (2018), no. 11, 965, arXiv:1804.05252.

[14] M. I. Abdulhamid et al., “Azimuthal correlations of high transverse momentum jets at next-to-leading order in the parton branching method”, *Eur. Phys. J. C* **82** (2022), no. 1, 36, arXiv:2112.10465.

[15] R. Angeles-Martinez et al., “Transverse Momentum Dependent (TMD) parton distribution functions: status and prospects”, *Acta Phys. Polon. B* **46** (2015), no. 12, 2501, arXiv:1507.05267.

[16] J. Collins and J.-W. Qiu, “k_T factorization is violated in production of high-transverse-momentum particles in hadron-hadron collisions”, *Phys. Rev.* **D75** (2007) 114014, arXiv:0705.2141.

[17] W. Vogelsang and F. Yuan, “Hadronic Dijet Imbalance and Transverse-Momentum Dependent Parton Distributions”, *Phys. Rev. D* **76** (2007) 094013, arXiv:0708.4398.

[18] T. C. Rogers and P. J. Mulders, “No Generalized TMD-Factorization in Hadro-Production of High Transverse Momentum Hadrons”, *Phys.Rev.* **D81** (2010) 094006, arXiv:1001.2977.

[19] F. Hautmann et al., “Soft-gluon resolution scale in QCD evolution equations”, *Phys. Lett. B* **772** (2017) 446, arXiv:1704.01757.

[20] F. Hautmann et al., “Collinear and TMD quark and gluon densities from Parton Branching solution of QCD evolution equations”, *JHEP* **01** (2018) 070, arXiv:1708.03279.

[21] J. Alwall et al., “The automated computation of tree-level and next-to-leading order differential cross sections, and their matching to parton shower simulations”, *JHEP* **1407** (2014) 079, arXiv:1405.0301.

[22] V. N. Gribov and L. N. Lipatov, “Deep inelastic ep scattering in perturbation theory”, *Sov. J. Nucl. Phys.* **15** (1972) 438–450. [Yad. Fiz.15,781(1972)].

[23] L. N. Lipatov, “The parton model and perturbation theory”, *Sov. J. Nucl. Phys.* **20** (1975) 94. [Yad. Fiz.20,181(1974)].

[24] G. Altarelli and G. Parisi, “Asymptotic freedom in parton language”, *Nucl. Phys. B* **126** (1977) 298.

[25] Y. L. Dokshitzer, “Calculation of the structure functions for Deep Inelastic Scattering and e^+e^- annihilation by perturbation theory in Quantum Chromodynamics.”, *Sov. Phys. JETP* **46** (1977) 641–653. [Zh. Eksp. Teor. Fiz.73,1216(1977)].

[26] A. Bermudez Martinez et al., "Collinear and TMD parton densities from fits to precision DIS measurements in the parton branching method", *Phys. Rev. D* **99** (2019) 074008, arXiv:1804.11152.

[27] ZEUS, H1 Collaboration, "Combination of measurements of inclusive deep inelastic $e^{\pm}p$ scattering cross sections and QCD analysis of HERA data", *Eur. Phys. J. C* **75** (2015) 580, arXiv:1506.06042.

[28] J. Alwall et al., "A standard format for Les Houches event files", *Comput. Phys. Commun.* **176** (2007) 300, arXiv:hep-ph/0609017.

[29] S. Baranov et al., "CASCADE3 A Monte Carlo event generator based on TMDs", *Eur. Phys. J. C* **81** (2021) 425, arXiv:2101.10221.

[30] G. Corcella et al., "HERWIG 6.5 release note", arXiv:hep-ph/0210213.

[31] G. Marchesini et al., "HERWIG: A Monte Carlo event generator for simulating hadron emission reactions with interfering gluons. Version 5.1 - April 1991", *Comput. Phys. Commun.* **67** (1992) 465–508.

[32] M. Cacciari, G. P. Salam, and G. Soyez, "The anti-k_t jet clustering algorithm", *JHEP* **04** (2008) 063, arXiv:0802.1189.

[33] M. Cacciari, G. P. Salam, and G. Soyez, "FastJet User Manual", *Eur. Phys. J. C* **72** (2012) 1896, arXiv:1111.6097.

[34] NNPDF Collaboration, "Parton distributions for the LHC Run II", *JHEP* **04** (2015) 040, arXiv:1410.8849.

[35] CMS Collaboration, "Event generator tunes obtained from underlying event and multiparton scattering measurements", *Eur. Phys. J. C* **76** (2016) 155, arXiv:1512.00815.

[36] J. Bellm et al., "Parton Shower Uncertainties with Herwig 7: Benchmarks at Leading Order", arXiv:1605.01338.